

# Imaging Artifacts of Liquid Embolic Agents on Conventional CT in an Experimental in Vitro Model

 N. Schmitt,  R.O. Flocu,  D. Paech,  R.A. El Shafie,  F. Seker,  M. Bendszus,  M.A. Möhlenbruch, and  D.F. Vollherbst

## ABSTRACT

**BACKGROUND AND PURPOSE:** Endovascular embolization using liquid embolic agents is a safe and effective treatment option for AVMs and dural arteriovenous fistulas. The aim of this study was to assess the degree of artifact inducement by the most frequently used liquid embolic agents in conventional CT in an experimental in vitro model.

**MATERIALS AND METHODS:** Dimethyl-sulfoxide-compatible tubes were filled with the following liquid embolic agents ( $n=10$ , respectively): Onyx 18, all variants of Squid, PHIL 25%, PHIL LV, and *n*-BCA mixed with iodized oil. After inserting the tubes into a CT imaging phantom, we acquired images. Artifacts were graded quantitatively by the use of Hounsfield units in a donut-shaped ROI using a customized software application that was specifically designed for this study and were graded qualitatively using a 5-point scale.

**RESULTS:** Quantitative and qualitative analyses revealed the most artifacts for Onyx 18 and the least artifacts for *n*-BCA, PHIL 25%, and PHIL LV. Squid caused more artifacts compared with PHIL, both for the low-viscosity and for the extra-low-viscosity versions (eg, quantitative analysis, Squid 18: mean  $\pm$  SD,  $30.3 \pm 9.7$  HU versus PHIL 25%: mean  $\pm$  SD,  $10.6 \pm 0.8$  HU;  $P < .001$ ). Differences between the standard and low-density variants of Squid were observed only quantitatively for Squid 12. There were no statistical differences between the different concentrations of Squid and PHIL.

**CONCLUSIONS:** In this systematic in vitro analysis investigating the most commonly used liquid embolic agents, relevant differences in CT imaging artifacts could be demonstrated. Ethylene-vinyl alcohol-based liquid embolic agents induced more artifacts compared with liquid embolic agents that use iodine as a radiopaque component.

**ABBREVIATIONS:** EVOH = ethylene-vinyl alcohol; LD = low density; LEA = liquid embolic agent; LV = low viscosity; MITK = Medical Imaging Interaction Toolkit; *n*-BCA = *n*-butyl cyanoacrylate

In addition to microneurosurgery and stereotactic radiation therapy, endovascular embolization using liquid embolic agents (LEAs) is an effective treatment mode for the therapy of cerebral AVMs or cranial dural AVFs. Depending on the type and extension of the vascular malformation, the endovascular treatment can be performed either alone or in combination with one of the other methods.<sup>1</sup>

For the treatment of such vascular malformations, several LEAs, each with different properties, are currently available on the market. The most commonly used nonadhesive material is Onyx (Medtronic), a LEA consisting of an ethylene-vinyl alcohol (EVOH) copolymer, dimethyl-sulfoxide, and tantalum powder. Numerous studies have demonstrated the effectiveness and safety of Onyx for the treatment of vascular malformations.<sup>2,3</sup> Another LEA, also based on EVOH and tantalum powder is Squid (Balt Extrusion), which has been commercially available since 2012, with its low-viscosity versions, Squid 18 and Squid 18 low density (LD), and its extra-low-viscosity versions, Squid 12 and Squid 12 LD. For adequate visibility during embolization, radiopacity for these 5 nonadhesive agents is induced by the admixed tantalum powder.<sup>4,5</sup> The difference between Onyx and Squid is that for Squid, the tantalum powder consists of a smaller “micronized” grain size, which is aimed at enhancing the homogeneity in radiopacity and improving the visibility during longer injections times.<sup>5</sup> The aim of the LD variants of Squid is to reduce the

Received June 10, 2020; accepted after revision August 14.

From the Departments of Neuroradiology (N.S., F.S., M.B., M.A.M., D.F.V.) and Radiation Oncology (R.O.F., R.A.E.S.), Heidelberg University Hospital, Heidelberg, Germany; Medical and Biological Informatics (R.O.F.), and Department of Radiology (D.P.), German Cancer Research Center, Heidelberg, Germany; and Heidelberg Institute for Radiation Oncology and National Center for Radiation Research in Oncology (R.O.F.), Heidelberg, Germany.

This work received technical support from Balt and MicroVention.

The authors had full control of the data and its analysis throughout the study. No outside interests have influenced our results.

Please address correspondence to Dominik F. Vollherbst, MD, Department of Neuroradiology, Heidelberg University Hospital, INF 400, 69120 Heidelberg, Germany; e-mail: Dominik.Vollherbst@med.uni-heidelberg.de

<http://dx.doi.org/10.3174/ajnr.A6867>



**FIG 1.** Schematic illustration of the donut-shaped ROI created by the MITK with an inner radius of 6 mm and an outer radius of 26 mm. The tube filled with the LEA of interest was placed centrally with a radius equal to the radius of the donut hole. For each tube, the measurement was performed with an ROI in 5 different positions according to the length of the LEA cast.

radiopacity to improve the differentiation of the embolized and nonembolized parts of the malformation without influencing the embolic properties.

A further commercially available LEA, which was introduced recently, is Precipitating Hydrophobic Injectable Liquid (PHIL; MicroVention) with its low-viscosity version PHIL 25% and its extra-low-viscosity version PHIL low viscosity (LV).<sup>6,7</sup> PHIL is a nonadhesive precipitating embolic agent that consists of 2 specific copolymers [poly(lactide-co-glycolide) and polyhydroxyethylmethacrylate] as its active ingredients and triiodophenol (an iodine compound), which is covalently bound to the copolymers, thus enabling the intrinsic radiopacity of PHIL.<sup>8,9</sup>

Before the introduction of these nonadhesive embolic agents, which are all based on the mechanism of precipitation, liquid embolization was predominantly performed with adhesive cyanoacrylates. The active component of cyanoacrylates is *n*-butyl cyanoacrylate (*n*-BCA), which is available in different chemical compositions and is normally mixed with iodized oil for adequate radiopacity. Even though the use of cyanoacrylates has decreased since the introduction of the above-mentioned nonadhesive LEAs,<sup>10,11</sup> *n*-BCA and its derivatives are still used effectively in particular situations, for example, for the treatment of high-flow malformations and for specific techniques such as the pressure cooker technique.<sup>12</sup>

A major drawback of LEAs is imaging artifacts, predominantly in CT.<sup>13,14</sup> Because intracranial vascular malformations are associated with an increased risk of peri- and postprocedural hemorrhage, embolization-related artifacts can represent a crucial obstacle in the detection of intracranial blood during or after embolization in CT.<sup>15</sup> Furthermore, some vascular malformations, especially complex AVMs, cannot be completely occluded by endovascular means, requiring subsequent radiation therapy afterward.<sup>1</sup> The corresponding treatment-planning recordings are usually based on conventional CT imaging.<sup>16</sup> Thus, embolization-related artifacts represent another substantial drawback for adequate and safe treatment planning of further radiation projects.<sup>17-19</sup>

Systematic data for imaging artifacts of LEAs is rare. To our knowledge, to date, only a few reports with low case numbers that investigated the imaging artifacts of the above-mentioned

LEAs (Onyx versus PHIL and Onyx versus Squid) are available.<sup>13,14</sup> The differences in CT artifacts between Squid and PHIL, between nonadhesive LEAs and *n*-BCA, and imaging artifacts of the extra-low viscosity LEAs Squid 12 and PHIL LV were not the focus of research until now.

The aim of the present study was the systematic assessment of artifacts of the most commonly used LEAs in conventional CT in an in vitro tube model.

## MATERIALS AND METHODS

### Sample Preparation

Dimethyl-sulfoxide-compatible tubes, with a length of 30 mm, an outer diameter of 8 mm, and an inner diameter of 4 mm, were used for this study. In a first step, the tubes were flushed with warm saline (38.0°C; NaCl, 0.9%). As is recommended for clinical use, each of the examined LEAs was prepared in accordance with the manufacturer's instructions. Afterward, complete filling of the tubes was performed with Onyx 18, all variants of Squid (Squid 18, Squid 18 LD, Squid 12, and Squid 12 LD), PHIL 25%, PHIL LV, and *n*-BCA mixed with iodized oil (Lipiodol Ultra-Fluid; Guerbet) in a ratio of 1:1. Ten tubes were filled and investigated per LEA. As a control group, tubes ( $n = 10$ ) were filled with saline 0.9%.

### Imaging

To ensure a homogeneous distribution of the LEAs within the tubes, we obtained a single-shot x-ray immediately after filling. Directly afterwards, the filled tubes were inserted into a custom-made CT phantom, as previously described by Daubner et al.<sup>20</sup> The average density was similar to that of brain tissue (mean,  $33.9 \pm .9$  HU). The beam path for all CT scans was orthogonal to the LEA-filled tubes, to ensure an optimal spread of artifacts. Conventional CT was performed with standard settings according to clinical practice with a tube voltage of 120 kV and a tube current of 20 mAs on a 64-section multidetector, single-source scanner (Somatom Definition AS; Siemens). A standard imaging protocol was used according to recommendations by the manufacturer and used as in clinical routine. In a next step, all images were reconstructed with a J40s kernel at a section thickness of 4 mm.

### Quantitative Analysis of the Imaging Artifacts

Quantitative analysis of the LEA-related artifacts was conducted with the Medical Imaging Interaction Toolkit (MITK, Germany Cancer Research Center, Division of Medical Image Computing, Heidelberg, Germany; <https://docs.mitk.org/2018.04/>) in the axial plane.<sup>21</sup> Therefore, a customized feature of the MITK software was specifically implemented for this study. This feature allowed us to place a standardized ROI with a donut-shaped configuration adjacent to and surrounding the center of each filled tube. This standardized ROI with a donut-shaped configuration ensured that the LEA-filled tube was excluded from the analysis, thus preventing distortion of the artifacts by the LEA. The outer radius of the donut-shaped ROI was set at 26 mm, while the inner radius was set at 6 mm, whereas the tube itself, with an outer diameter of 8 mm, was positioned at the center of the donut hole (Fig 1). For an adequate placement of the ROI, the width and the level of the window were adjusted manually for each measurement. According to the length of the LEA cast, 5 ROIs were set in different positions with a distance of 4 mm along the tube to ensure that all artifacts were taken into account.

The degree of imaging artifact production was assessed by calculating the SD of the Hounsfield units in the ROI, as described previously.<sup>13,14</sup> Because streak artifacts in conventional CT usually consist of alternating areas of very high- and very low-density, respectively, using the SD as a measurement for the degree of artifact production has the advantage of not being canceled out, as might be the case for the mean of the Hounsfield unit values.<sup>19</sup>

### Qualitative Analysis of the Imaging Artifacts

Qualitative analyses of the conventional CT images were performed on a PACS workstation by 2 different readers (reader 1 with 4 years; reader 2 with 9 years of experience in diagnostic imaging, respectively), blinded to the type of LEA and saline. The reconstructed

images were all reviewed in slices with a thickness of 4 mm in the axial plane in a standard CT brain window with a width of 80 and a level of 40. The observers were not allowed to adjust the window.

The degree of artifacts was graded on a 5-point scale:<sup>22</sup> 1) severe artifacts, 2) marked artifacts, 3) moderate artifacts, 4) minor artifacts, and 5) no artifacts.

### Statistics

GraphPad Prism software (Version 8.4.2; GraphPad Software) was used for statistical analysis. The interreader agreement for the qualitative image analysis was assessed using an unweighted Cohen  $\kappa$  coefficient.<sup>23</sup> The  $\kappa$  values were interpreted as follows:  $\leq 0.20$ , poor agreement; 0.21–0.40, fair agreement; 0.41–0.60, moderate agreement; 0.61–0.80, good agreement; and 0.81–1.00, very good agreement.<sup>24</sup> Data are presented as mean  $\pm$  SD. To evaluate statistical differences among the study groups, we performed the Kruskal-Wallis test. To test for differences among the individual study groups, we used the Dunn test for multiple comparisons using statistical hypothesis testing as a post hoc test. The Dunn test was performed only for corresponding LEA variants, low-viscosity variants (Onyx 18 versus Squid 18 versus PHIL 25%), extra-low-viscosity variants (Squid 12 versus PHIL LV), and LD variants of Squid (Squid 18 versus Squid 18 LD and Squid 12 versus Squid 12 LD), to reduce the number of statistical tests. *n*-BCA and the control group were compared with Onyx 18 and all Squid and PHIL variants, respectively. The significance level was defined at  $P < .05$ .

### RESULTS

The results of the quantitative image analysis are summarized in Tables 1 and 2, and Fig 2. Representative CT images of the examined LEAs are demonstrated in Fig 3. The results of the qualitative analysis are demonstrated in Fig 4 and Table 3. There was very good agreement for the qualitative grading of artifacts in conventional CT ( $\kappa = 0.954$ ; range, 0.902–1.0). The Kruskal-Wallis test showed a statistically significant difference ( $P < .001$ ) in the degree of artifacts among all study groups of the quantitative and qualitative analyses. Regarding the low-viscosity LEAs, Onyx 18 and Squid 18 induced a higher degree of artifacts compared with PHIL 25% for both the quantitative and qualitative analyses (eg,  $P < .001$  for Onyx 18 and  $P < .001$  for Squid 18 for the quantitative analysis). No difference was observed between Onyx 18 and Squid 18 (eg,  $P > .999$  for the qualitative analysis). For the extra-low-viscosity LEAs in both analyses, more severe artifacts were caused by Squid 12 compared with PHIL LV (eg,  $P < .001$  for the quantitative analysis). Compared with *n*-BCA, only the standard versions

**Table 1: Summary of the quantitative imaging analysis**

Liquid Embolic Agent	SD of Donut-Shaped ROI	P Value <sup>a</sup>
Onyx 18	56.6 $\pm$ 20.1 HU	
Squid 18	30.3 $\pm$ 9.7 HU	
Squid 18 LD	18.5 $\pm$ 6.8 HU	
Squid 12	33.4 $\pm$ 17.3 HU	
Squid 12 LD	19.4 $\pm$ 7.7 HU	$P < .001$
PHIL 25%	10.6 $\pm$ 0.8 HU	
PHIL LV	10.1 $\pm$ 0.9 HU	
<i>n</i> -BCA/iodized oil	11.9 $\pm$ 1.0 HU	
Saline	5.1 $\pm$ 0.1 HU	

<sup>a</sup>Kruskal-Wallis test; for the *P* values of the post hoc analysis, see Table 2.

**Table 2: Summary of the results of the post hoc Dunn test for the quantitative analysis**

Liquid Embolic Agent	Onyx 18	Squid 18	Squid 18 LD	Squid 12	Squid 12 LD	PHIL 25%	PHIL LV	<i>n</i> -BCA/Iodized Oil
Saline	$P < .001^a$	$P < .001^a$	$P < .001^a$	$P < .001^a$	$P < .001^a$	$P = .001^a$	$P = .034^a$	$P < .001^a$
<i>n</i> -BCA/iodized oil	$P < .001^a$	$P < .001^a$	$P = .106$	$P < .001^a$	$P = .468$	$P = .987$	$P = .096$	
PHIL LV	NA	NA	NA	$P < .001$	NA	$P > .999$		
PHIL 25%	$P < .001^a$	$P < .001^a$	NA	NA	NA			
Squid 12 LD	NA	NA	$P > .999$	$P = .013^a$				
Squid 12	NA	$P > .999$	NA					
Squid 18 LD	NA	$P = .057$						
Squid 18	$P = .118$							

**Note:**—NA indicates no *P* value available because the Dunn test was only performed for corresponding LEA variants.

<sup>a</sup>Statistical significance.



of the EVOH-based LEAs (Onyx 18, Squid 18, and Squid 12) showed more artifacts quantitatively and qualitatively (eg,  $P < .001$  for Onyx 18,  $P = .004$  for Squid 18, and  $P = .003$  for Squid 12 in qualitative statistics). The degree of artifacts was lowest for the saline-filled tubes (control group), reaching statistical significance in

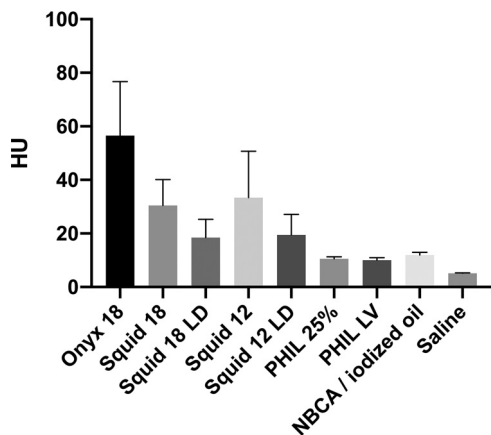


**FIG 2.** Illustration of the results of the quantitative image analysis. Different degrees of artifacts were observed among all study groups. Post hoc testing showed differences among the different types of LEAs (eg, Squid 18 versus PHIL 25% and Squid 12 versus PHIL LV). Bars indicate mean; whiskers, SD.

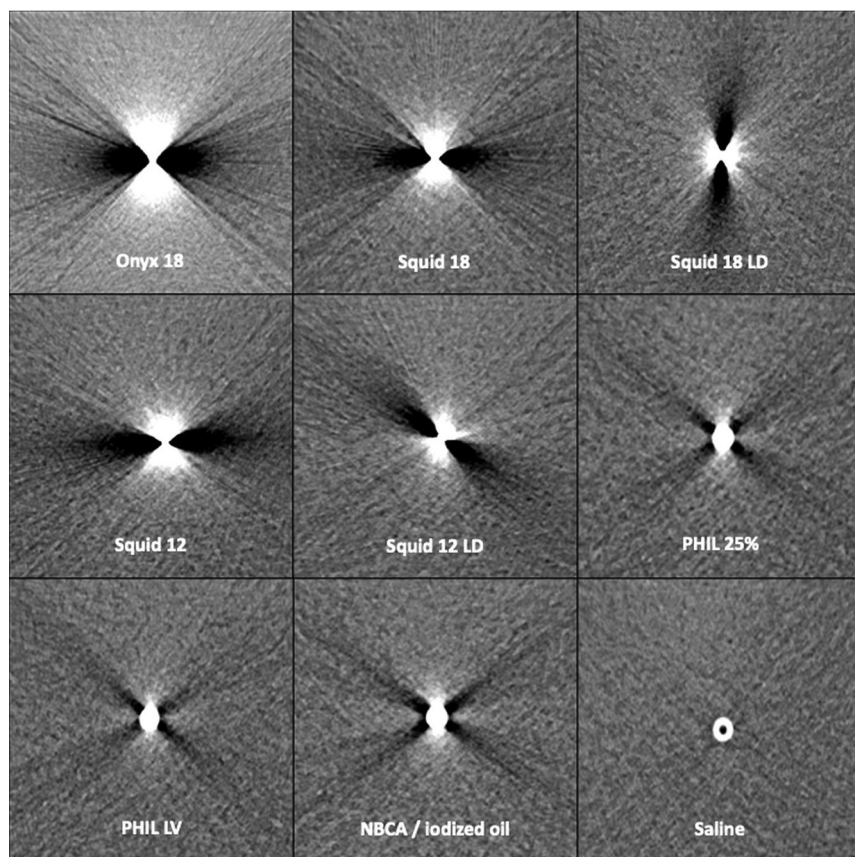


**FIG 3.** Representative CT images in the axial plane in a standard brain window with a width of 80 and a length of 40. Note the more severe artifacts for the EVOH-based LEAs (Onyx and Squid) and the relatively low degree of artifacts for LEAs that used iodine as a radiopaque component (PHIL and *n*-BCA/iodized oil).

all groups except for PHIL 25%, PHIL LV, and *n*-BCA in the qualitative analysis. When we compared the standard and the LD variants of Squid, the degree of artifacts tended to be lower for Squid 18 LD and Squid 12 LD; however, they were only statistically significant for quantitative analysis of Squid 12 ( $P = .013$ ). The versions of PHIL and Squid with different viscosities (eg, PHIL 25% versus PHIL LV and Squid 18 versus Squid 12) did not show significant differences.

## DISCUSSION

Endovascular embolization using LEAs is an established treatment option for AVMs and DAVFs.<sup>1</sup> Currently, various embolic agents are commercially available, each with specific properties.<sup>25,26</sup> One of the main disadvantages of LEAs is the generation of imaging artifacts in peri- and postprocedural CT.<sup>4,13</sup>

In the present study, we demonstrated that the imaging artifacts induced by LEAs vary to a substantial degree. EVOH-based LEAs induce more artifacts compared with a copolymer-based LEA, which uses covalently bound iodine as a radiopaque component, while *n*-BCA and iodized oil induce only minor artifacts on conventional CT.

To date, to the best of our knowledge, only 2 studies have investigated the difference in CT imaging artifacts of nonadhesive liquid embolic agents.<sup>13,14</sup> Vollherbst et al<sup>13</sup> compared the imaging artifacts of Onyx and PHIL in an exper-

imental animal study and reported a higher degree of artifacts for Onyx 18 compared with PHIL 25% on conventional CT. In an experimental in vitro tube model, Pop et al<sup>14</sup> investigated Onyx and Squid regarding their production of CT imaging artifacts. Their results demonstrated fewer imaging artifacts for all variants of Squid compared with Onyx 18 as well as for the LD variants compared with their normal-density counterparts on conventional CT. Furthermore, they observed lower artifacts for Squid 18 than for Squid 12.<sup>14</sup>

Systematic analyses of imaging artifacts on conventional CT between Squid and PHIL, between nonadhesive LEAs and *n*-BCA, as well as artifacts of the extra-low-viscosity LEAs Squid 12 and PHIL LV have not been reported until now.

Regarding the present study, there are 3 major advantages: 1) The customized donut-shaped ROI was used for the image analysis; 2) all LEAs that are commonly used for embolization of cerebral vascular malformations were investigated in parallel; and 3) there was a high case number of the experiments per study group.

In both aforementioned studies, the analysis was performed by setting a round or rectangular ROI in the direct vicinity of the filled tubes without taking all artifacts into account. Using a customized feature of the MITK software, which was specifically designed for the present study, allowed us to set a standardized donut-shaped ROI adjacent to and surrounding the center of each filled tube. This approach has the major advantage of considering all artifacts around the liquid embolic agent and at the same time not taking the filled tubes into account. Accordingly, this technique of quantitative analysis enabled a more precise evaluation as well as a more adequate comparability of the CT imaging artifacts of the different study groups. To ensure that the artifacts in all CT image slices were taken into account, we placed 5 ROIs according to the length of the cast of each tube for each of the different LEAs.

Furthermore, previous studies compared only the imaging artifacts of Onyx versus PHIL and Onyx versus Squid while performing a relatively low number of experiments per LEA. In the present study, a systematic assessment of 8 commonly used LEAs was performed with 10 experiments per study group. In addition, the imaging artifacts of the different LEAs were compared with saline-filled tubes serving as a control group, while in the 2 above-mentioned previous studies, no control groups were included.

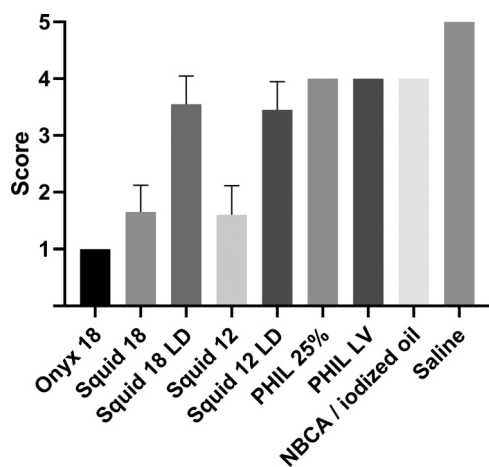


**FIG 4.** Illustration of the results of the qualitative image analysis using a 5-point scale. Different degrees of artifacts were observed among all study groups using the Dunn test for multiple comparisons with statistical hypothesis testing. Bars indicate mean; whiskers, SD. Five-point scale: 1) severe artifacts, 2) marked artifacts, 3) moderate artifacts, 4) minor artifacts, and 5) no artifacts.

The low degree of artifact production of PHIL compared with the EVOH-based LEAs Onyx and Squid can be explained by the chemical elements that cause radiopacity. The atomic number of the admixed radiopaque materials seems to have a major impact on the production of imaging artifacts predominantly caused by beam-hardening on conventional CT.<sup>19</sup> The higher atomic number of tantalum (atomic number 73) as part of Onyx and Squid leads to more artifacts compared with iodine (atomic number 53) as part of PHIL.

In the experimental study of Pop et al,<sup>14</sup> Onyx 18 produced more artifacts than Squid 18. In our study, there was also a tendency toward more artifacts for Onyx 18, however, without reaching statistical significance. As initially indicated, the LD variants of Squid mainly aim to improve the x-ray visibility of the embolized and nonembolized portions of vascular malformations during the embolization procedure. Comparing the normal-density variants and the LD variants of Squid, we observed a lower degree of imaging artifacts for the LD variants; however, the level of statistical significance was reached only for Squid 12 in the quantitative analysis ( $P = .013$ ). Because the LD variants contain a 30% lower concentration of tantalum, the findings of our study suggest that this effect might be lower than expected and that the concentration of tantalum has only a moderate impact on artifacts in CT imaging.

The artifacts of cyanoacrylates have not been specifically investigated until now. Because *n*-BCA is not inherently visible, in clinical practice it is mixed with iodized oil for adequate visibility.<sup>27</sup> Accordingly, imaging artifacts of this LEA are caused by the iodized oil component and not by *n*-BCA. Iodized oil, which is composed of iodine combined with ethyl esters of fatty acids of poppyseed oil, affects not only the radiopacity of the mixture but also the embolization properties: the higher the concentration of iodized oil, the less viscous the embolic mixture. In our systematic investigation, *n*-BCA mixed with iodized oil produced less CT artifacts than the EVOH-based LEAs, but there were only statistical differences for Onyx 18 and the standard versions of Squid. In clinical practice, the concentration that was investigated in the present study (1:1) is relatively high and is predominantly used for high-flow shunts or for special techniques, such as the pressure cooker technique. For the effective embolization of larger vascular malformations, a lower viscosity of the LEA and therefore a higher concentration of iodized oil are usually needed.<sup>12</sup> For *n*-BCA/iodized mixtures with higher concentrations of iodized oil, higher levels of artifacts can be expected.

**Table 3: Summary of the results of the post hoc Dunn test for the qualitative analysis**

Liquid Embolic Agent	Onyx 18	Squid 18	Squid 18 LD	Squid 12	Squid 12 LD	PHIL 25%	PHIL LV	<i>n</i> -BCA/Iodized Oil
Saline	$P < .001^a$	$P < .001^a$	$P = .022^a$	$P < .001^a$	$P = .009^a$	$P = .665$	$P = .665$	$P = .665$
<i>n</i> -BCA/iodized oil	$P < .001^a$	$P = .004^a$	$P > .999$	$P = .003^a$	$P > .999$	$P > .999$	$P > .999$	
PHIL LV	NA	NA	NA	$P = .003^a$	NA	$P > .999$		
PHIL 25%	$P < .001^a$	$P = .004^a$	NA	NA	NA			
Squid 12 LD	NA	NA	$P > .999$	$P = .311$				
Squid 12	NA	$P > .999$	NA					
Squid 18 LD	NA	$P = .201$						
Squid 18	$P > .999$							

**Note:**—NA indicates no *P* value available because the Dunn test was performed for only corresponding LEA variants.

<sup>a</sup>Statistical significance.

We acknowledge that this study has some limitations. In general, the transferability of an in vitro model to clinical practice is limited. While the tube model allowed a highly standardized analysis and comparison of artifacts, a more complex 3D model would have better resembled a human vascular malformation. Only 1 tube size and only 1 mixture of *n*-BCA/iodized oil were investigated, but different tube sizes and different concentrations of *n*-BCA/iodized oil may result in different findings. Furthermore, the tubes were not flushed continuously with saline during the injection of the LEAs, and this feature may have an influence on the results.

## CONCLUSIONS

In investigating the most commonly used LEAs, marked differences in CT imaging artifacts could be demonstrated. The EVOH-based LEAs Onyx and Squid induced more artifacts compared with PHIL. *n*-BCA mixed with iodized oil induced only minor artifacts in conventional CT.

Disclosures: Niclas Schmitt—*OTHER RELATIONSHIPS*: Regarding our work, there was technical support by Balt and MicroVention. The authors had full control of the data and its analysis throughout the study. No outside interests have influenced our results. Daniel Paech—*UNRELATED: Grants/Grants Pending*: German Research Foundation grant\*; *Travel/Accommodations/Meeting Expenses Unrelated to Activities Listed*: Siemens, *Comments*: travel support to CEST Workshop, Beijing 2018. Martin Bendszus—*UNRELATED: Board Membership*: Data and Safety Monitoring Board for Vascular Dynamics, Boehringer; *Consultancy*: Codman, Braun; *Grants/Grants Pending*: German Research Foundation, European Union, Hopp Foundation, Novartis, Siemens, Stryker, Medtronic, Guerbet\*; *Payment for Lectures Including Service on Speakers Bureaus*: Novartis, Teva Pharmaceutical Industries, Codman, Guerbet, Merck, Grifols, Bayer AG, Leverkusen, Germany. Markus A. Möhlenbruch—*UNRELATED: Consultancy*: Medtronic, MicroVention, Stryker\*; *Grants/Grants Pending*: Balt, MicroVention, Medtronic, Stryker\*; *Payment for Lectures Including Service on Speakers Bureaus*: MicroVention, Medtronic, Stryker.\* Dominik F. Vollherbst—*UNRELATED: Travel/Accommodations/Meeting Expenses Unrelated to Activities Listed*: MicroVention, Stryker, *Comments*: travel support\*; *OTHER RELATIONSHIPS*: This study was technically supported by Balt and MicroVention (provision of the embolic agents). \*Money paid to institution.

## REFERENCES

- Friedlander RM. **Clinical practice: arteriovenous malformations of the brain.** *N Engl J Med* 2007;356:2704–12 [CrossRef Medline](#)
- van Rooij WJ, Sluzewski M, Beute GN. **Brain AVM embolization with Onyx.** *AJNR Am J Neuroradiol* 2007;28:172–77; discussion 178 [Medline](#)
- Weber W, Kis B, Siekmann R, et al. **Endovascular treatment of intracranial arteriovenous malformations with Onyx: technical aspects.** *AJNR Am J Neuroradiol* 2007;28:371–77 [Medline](#)
- Saatci I, Cekirge HS, Ciceri EF, et al. **CT and MR imaging findings and their implications in the follow-up of patients with intracranial aneurysms treated with endosaccular occlusion with Onyx.** *AJNR Am J Neuroradiol* 2003;24:567–78 [Medline](#)
- Mason JR, Dodge C, Benndorf G. **Quantification of tantalum sedimentation rates in liquid embolic agents.** *Interv Neuroradiol* 2018;24:574–79 [CrossRef Medline](#)
- Varadharajan S, Ramalingaiah AH, Saini J, et al. **Precipitating hydrophobic injectable liquid embolization of intracranial vascular shunts: initial experience and technical note.** *J Neurosurg* 2018;129:1217–22 [CrossRef Medline](#)
- Vollherbst DF, Otto R, Hantz M, et al. **Investigation of a new version of the liquid embolic agent PHIL with extra-low-viscosity in an endovascular embolization model.** *AJNR Am J Neuroradiol* 2018;39:1696–1702 [CrossRef Medline](#)
- Vollherbst DF, Sommer CM, Ulfert C, et al. **Liquid embolic agents for endovascular embolization: evaluation of an established (Onyx) and a novel (PHIL) embolic agent in an in vitro AVM model.** *AJNR Am J Neuroradiol* 2017;38:1377–82 [CrossRef Medline](#)
- Vollherbst DF, Otto R, von Deimling A, et al. **Evaluation of a novel liquid embolic agent (precipitating hydrophobic injectable liquid (PHIL)) in an animal endovascular embolization model.** *J Neurointerv Surg* 2018;10:268–74 [CrossRef Medline](#)
- Elsenousi A, Aletich VA, Alaraj A. **Neurological outcomes and cure rates of embolization of brain arteriovenous malformations with *n*-butyl cyanoacrylate or Onyx: a meta-analysis.** *J Neurointerv Surg* 2016;8:265–72 [CrossRef Medline](#)
- Gross BA, Albuquerque FC, Moon K, et al. **Evolution of treatment and a detailed analysis of occlusion, recurrence, and clinical outcomes in an endovascular library of 260 dural arteriovenous fistulas.** *J Neurosurg* 2017;126:1884–93 [CrossRef Medline](#)
- Chapot R, Stracke P, Velasco A, et al. **The pressure cooker technique for the treatment of brain AVMs.** *J Neuroradiol* 2014;41:87–91 [CrossRef Medline](#)
- Vollherbst DF, Otto R, Do T, et al. **Imaging artifacts of Onyx and PHIL on conventional CT, cone-beam CT and MRI in an animal model.** *Interv Neuroradiol* 2018;24:693–701 [CrossRef Medline](#)
- Pop R, Mertzt L, Ilyes A, et al. **Beam hardening artifacts of liquid embolic agents: comparison between Squid and Onyx.** *J Neurointerv Surg* 2019;11:706–09 [CrossRef Medline](#)
- Lv X, Wu Z, Li Y, et al. **Hemorrhage risk after partial endovascular *n*-BCA and Onyx embolization for brain arteriovenous malformation.** *Neurol Res* 2012;34:552–56 [CrossRef Medline](#)
- Pereira GC, Traughber M, Muzic RF Jr. **The role of imaging in radiation therapy planning: past, present, and future.** *Biomed Res Int* 2014;2014:231090 [CrossRef Medline](#)
- Shtraus N, Schifter D, Corn BW, et al.  **radiosurgical treatment planning of AVM following embolization with Onyx: possible dosage error in treatment planning can be averted.** *J Neurooncol* 2010;98:271–76 [CrossRef Medline](#)
- Roberts DA, Balter JM, Chaudhary N, et al. **Dosimetric measurements of Onyx embolization material for stereotactic radiosurgery.** *Med Phys* 2012;39:6672–81 [CrossRef Medline](#)
- Giantsoudi D, De Man B, Verburg J, et al. **Metal artifacts in computed tomography for radiation therapy planning: dosimetric effects and impact of metal artifact reduction.** *Phys Med Biol* 2017;62:R49–80 [CrossRef Medline](#)
- Daubner D, Spieth S, Cerhova J, et al. **Measuring ventricular width on cranial computed tomography: feasibility of dose reduction in a custom-made adult phantom.** *Rofo* 2016;188:73–81 [CrossRef Medline](#)
- Nolden M, Zelzer S, Seitel A, et al. **The Medical Imaging Interaction Toolkit: challenges and advances: 10 years of open-source development.** *Int J Comput Assist Radiology Surg* 2013;8:607–20 [CrossRef Medline](#)
- Weiß J, Schabel C, Bongers M, et al. **Impact of iterative metal artifact reduction on diagnostic image quality in patients with dental hardware.** *Acta Radiol* 2017;58:279–85 [CrossRef Medline](#)
- Cohen J. **A coefficient of agreement for nominal scales.** *Educ Psychol Meas* 1960;20:37–46 [CrossRef](#)
- Altman DG. *Practical Statistics for Medical Research.* CRC Press; 1990
- Gross BA, Du R. **Diagnosis and treatment of vascular malformations of the brain.** *Curr Treat Options Neurol* 2014;16:279 [CrossRef Medline](#)
- Ramos S, Bortolotti C, Lanzino G. **Endovascular management of intracranial dural arteriovenous fistulae.** *Neurosurg Clin N Am* 2014;25:539–49 [CrossRef Medline](#)
- Stoesslein F, Ditscherlein G, Romaniuk PA. **Experimental studies on new liquid embolization mixtures (histoacryl-lipiodol, histoacryl-panthopaque).** *Cardiovasc Intervent Radiol* 1982;5:264–67 [CrossRef Medline](#)